Suppression of chaos by weak resonant excitations in a nonlinear oscillator with a non-symmetric potential

Grzegorz Litak, [a,1] Arkadiusz Syta, [b] Marek Borowiec [a]

[a] *Department of Applied Mechanics, Technical University of Lublin, Nadbystrzycka 36, PL-20-618 Lublin, Poland*

[b] *Department of Applied Mathematics, Technical University of Lublin, Nadbystrzycka 36, PL-20-618 Lublin, Poland*

Abstract

We examine the Mielnikov criterion for transition to chaos in case of one degree of freedom nonlinear oscillator with non symmetric potential. This system subjected to an external periodic force shows homoclinic transition from regular vibrations to chaos just before escape from the potential well. Especially we study the effect of a second resonant excitation with different phase on the system transition to chaos and propose a way of its control.

Key words: nonlinear vibration, Mielnikov criterion, bifurcation

1 Introduction

In this note shell examine vibration and show possible non feedback control of chaos in a simple, one degree of freedom, system subjected to external excitation with a non-symmetric stiffness given by the following equation:

$$\ddot{x} + \alpha\dot{x} + \delta x + \gamma x^2 = \mu\cos\omega t \tag{1}$$

where x is displacement $\alpha\dot{x}$ is linear damping, $\mu\cos\omega t$ is an external excitation while δx and γx^2 are linear and quadratic force terms:

$$F(x) = -\delta x - \gamma x^2. \tag{2}$$

[1] Fax: +48-815250808; E-mail: g.litak@pollub.pl (G. Litak), a.syta@pollub.pl (A. Syta), m.borowiec@pollub.pl (M. Borowiec)

Such systems, where quadratic term brakes the symmetry of a potential $V(x)$

$$V(x) \neq V(-x), \quad \text{and} \quad F(x) = -\frac{\partial V(x)}{\partial x}, \tag{3}$$

have been a subject of studies for many years [1,2,3,4,5,6,7,8,9,10]. These investigations were motivated by possible applications in description of physical systems mostly mechanical [1,3,7,8] and electrical systems [4]. They were also linked to possible metastable states of atoms and appear in problems within the elastic theory [2,11].

Systems which show homoclinic orbits and can be tackled analytically by perturbation methods. Namely by the Mielnikov method treating [12,13] excitation and damping terms in higher order. Such a treatment has been performed to selected problems with both symmetric and non-symmetric nonlinear forces [12,13,10] to derive the necessary condition for transition to chaotic motion. On the other regular and chaotic regions of solutions in system parameters can be stabilised by using an additional weak resonant excitation [14,15,16,17]. In this note we shell apply this method to the nonlinear system given by Eq. 1. Combined with the Mielnikov approach it will predict analytically the range of parameters which tam the chaotic behaviour. The paper is divided into 5 sections. After this introduction (Sec. 1) we perform Mielnikov analysis in Sec. 2. This discussion is followed by Sec. 3 where we include a week resonant excitation term. Its useful role in system control is shown there. The analytic predictions are confirmed by means of numerical simulations (Sec. 4). We ending up in Sec. 5 with conclusions.

2 Melnikov analysis

Note in this section we follow the discussion initiated by Thompson [2] where he derived the analytic formula for a critical amplitude of a nonlinear oscillator described by a similar (to our Eq. 1) equation. We decided to include this section as an important introductory part to our main results to be given in the next section.

Thus we start our study from the second order equation of motion 1. Transforming it into two differential equations of the first order we get

$$\begin{aligned} \dot{x} &= v \\ \dot{v} &= -\delta x - \gamma x^2 + \epsilon \left[-\tilde{\alpha} v + \tilde{\mu} \cos \omega t \right]. \end{aligned} \tag{4}$$

Looking for stable and unstable manifolds we have introduced small parameter

ϵ to the above equations and renormalised parameters $\tilde{\alpha}$ and $\tilde{\mu}$ via $\alpha = \epsilon\tilde{\alpha}$ and $\mu = \epsilon\tilde{\mu}$, respectively.

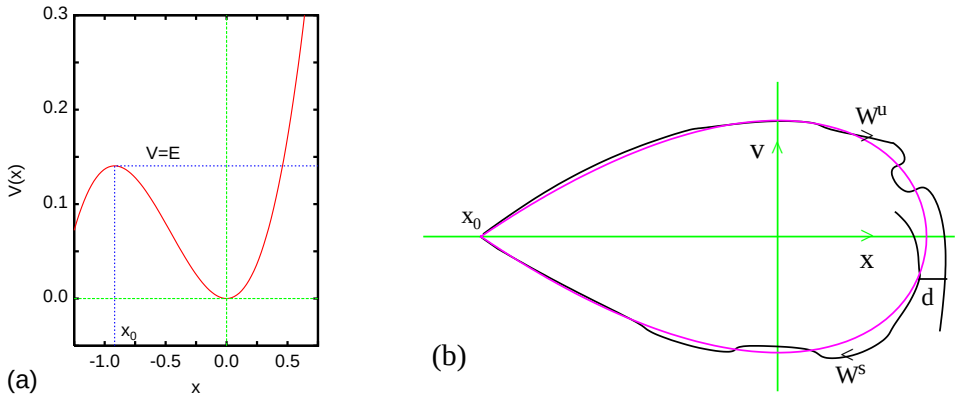

Fig. 1. (a) The potential well of the unperturbed Hamiltonian (Eq. 4) for $\delta = 1$ and $\gamma = 1.089$, the energy level $V = E$ corresponds to the Hamiltonian system with a tangent point at x_0 ; (b) stable W^S and unstable W^U manifolds for unperturbed (gray) and a damped and excited system (in black). The distance d between W^S and W^U can be described by Mielnikov function $M(t_0)$ (Eq. 9). Note x_0 indicates the local extremum of potential $V(x)$ (Fig. 1a) which simultaneously represents a saddle point in the phase plane (Fig. 1b).

The corresponding unperturbed Hamiltonian have the following form:

$$H^0 = \frac{v^2}{2} + V(x), \tag{5}$$

where

$$V(x) = \frac{\delta x^2}{2} + \frac{\gamma x^3}{3} \tag{6}$$

is the potential of a non-symmetric well plotted in Fig. 1a. This function has the local peak at the point

$$x_0 = -\frac{\delta}{\gamma}. \tag{7}$$

Existence of this point with a horizontal tangent make possible homoclinic bifurcations of the system i.e. potential transition from a regular to chaotic solution. After simple integration (Appendix A) we get homoclinic orbits (Fig. 1b) as:

$$x^* = \frac{\delta}{\gamma}\left(\frac{1}{2} - \frac{3}{2}\tanh^2\left(\frac{\sqrt{\delta}(t-t_0)}{2}\right)\right),$$

$$v^* = -\frac{3}{2}\frac{\delta\sqrt{\delta}\ \tanh\left(\frac{\sqrt{\delta}(t-t_0)}{2}\right)}{\gamma\ \cosh^2\left(\frac{\sqrt{\delta}(t-t_0)}{2}\right)}. \tag{8}$$

Note the characteristic saddle point x_0 is going to be reached in exactly defined albeit infinite time t corresponding to $+\infty$ and $-\infty$ for stable and unstable orbits, respectively.

In case of perturbed orbits W^S and W^U the distance between them is given by the Mielnicov function $M(t_0)$:

$$M(t_0) = \int_{-\infty}^{+\infty} h(x^*, v^*) \wedge g(x^*, v^*)\mathrm{d}t \tag{9}$$

where the corresponding differential forms h as the gradient of unperturbed Hamiltonian (Eq. 3) leading to equations of motion

$$\frac{\partial H^0}{\partial x} = -\dot{v}, \quad \frac{\partial H^0}{\partial v} = \dot{x}, \tag{10}$$

while g as its perturbation form of the above (Eq. 4):

$$\begin{aligned} h &= \left(\delta x + \gamma x^2\right)\mathrm{d}x + v\mathrm{d}v, \\ g &= \left(\tilde{\mu}\cos\omega\tau - \tilde{\alpha}v\right)\mathrm{d}x \end{aligned} \tag{11}$$

are defined on homoclinic manifold $(x, v) = (x^*, v^*)$ (Eq. 6, Fig. 2b). From the above (Eqs. 8-12) the Mielnikov integral is given by

$$M(t_0) = \int_{-\infty}^{+\infty} \mathrm{d}t \quad \left(\tilde{\mu}v^*\cos\left(\omega t\right) - \tilde{\alpha}v^{*2}\right) \tag{12}$$

After substituting $x^*(t)$ and $v^*(t)$ by formulae given in Eq. 8 and taking $\tau = \sqrt{\delta}t/2$ we get:

$$M(t_0) = -\frac{9}{2}\tilde{\alpha}\frac{\delta^2}{\gamma^2}\sqrt{\delta}I_1 - 3\tilde{\mu}\frac{\delta}{\gamma}I_2, \tag{13}$$

where

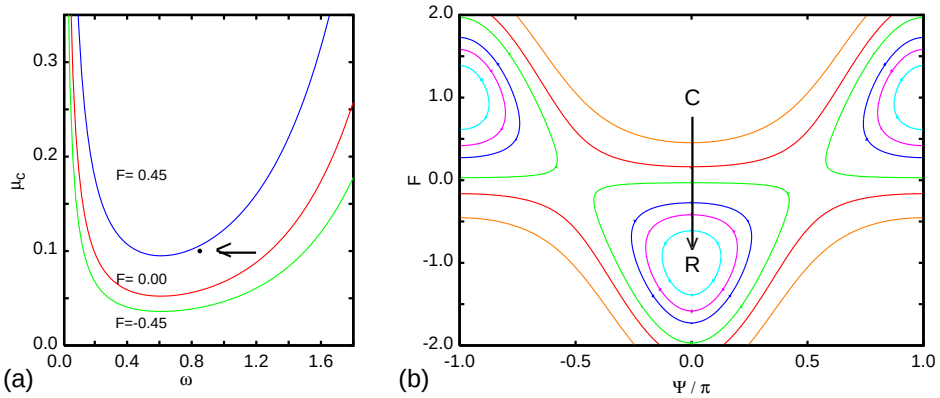

Fig. 2. (a) Critical value of μ_c plotted against ω for system parameters: $\gamma = 1.089$, $\delta = 1.0$. Control parameters were taken as $\Psi = \pi$ while $F = -0.45,\ 0.0$ and 0.45. The singular point below the upper curve corresponds to $\mu = 0.1$ and $\omega = 0.85$ used in numerical calculations - Figs. 4-5. (b) Phase diagram in a Ψ–F plane for a number of μ values, corresponding lines. The arrow indicate the direction of μ increase: $\mu = 0.04,\ 0.05,\ 0.06,\ 0.08,\ 0.10$ and 0.15, respectively. Here 'R' and 'C' denotes regions with regular and chaotic solutions.

$$I_1 = \int_{-\infty}^{+\infty} \mathrm{d}t \ \ \frac{\tanh^2 \tau}{\cosh^4 \tau}$$
$$I_2 = \int_{-\infty}^{+\infty} \mathrm{d}t \ \ \frac{\tanh \tau}{\cosh^2 \tau} \cos \frac{2\omega\,(\tau + \tau_0)}{\sqrt{\delta}} \tag{14}$$

After evaluation of these elementary integrals we get condition of homoclinic transition to chaos, corresponding to a horseshoe type of cross-section and can be written as:

$$\bigvee_{t_0} \quad M(t_0) = 0, \qquad \frac{\partial M(t_0)}{\partial t_0} \neq 0. \tag{15}$$

Evaluating above integrals (Eq. 14) after some lengthly algebra the last condition (Eq. 15) leads to a critical value of excitation amplitude μ_c for which

$$\mu_c = \frac{1}{5} \frac{\delta^2 \sqrt{\delta} \alpha}{\pi \omega^2 \gamma} \sinh\left(\frac{\omega \pi}{\sqrt{\delta}}\right). \tag{16}$$

As a result we get the critical amplitude μ_c versus frequency ω, which is plotted in Fig. 2(a) (the middle curve for $F = 0$). One should note here that the function has a local minimum at the point $\omega \approx 0.6$. Note that in spite of using $\cos(\omega t)$ in place of $\sin(\omega t)$, in the external excitation, discussed by Thompson [2] in the external excitation this result appears to be the same.

3 Effect of a weak resonant excitation

Let us consider an additional excitation term in starting equation (Eq. 1)

$$\ddot{x} + \alpha\dot{x} + \delta x + \gamma x^2 = \mu\cos(\omega t) + \mu F\cos(\omega t + \Psi), \tag{17}$$

where F is a scaling coefficient while Ψ represents a phase of a weak resonant excitation. Now instead of Eq. 4 one can separate unperturbed and small perturbation parts in the following differential equations of the first order:

$$\begin{aligned} \dot{x} &= v \\ \dot{v} &= -\delta x - \gamma x^2 + \epsilon\left[-\tilde{\alpha}v + \tilde{\mu}\cos(\omega t) + \tilde{\mu}F\cos(\omega t + \Psi)\right]. \end{aligned} \tag{18}$$

Now one can repeat most of calculations from the previous section assuming that the excitation term is composed of two parts. After simple algebra we get:

$$\cos(\omega t) + F\cos(\omega t + \Psi) = \sqrt{1 + F^2 + 2F\cos\Psi}\ \cos(\omega t + \alpha), \tag{19}$$

where

$$\alpha = \arctan\left(\frac{1 + F\cos\Psi}{F\sin\Psi}\right) \tag{20}$$

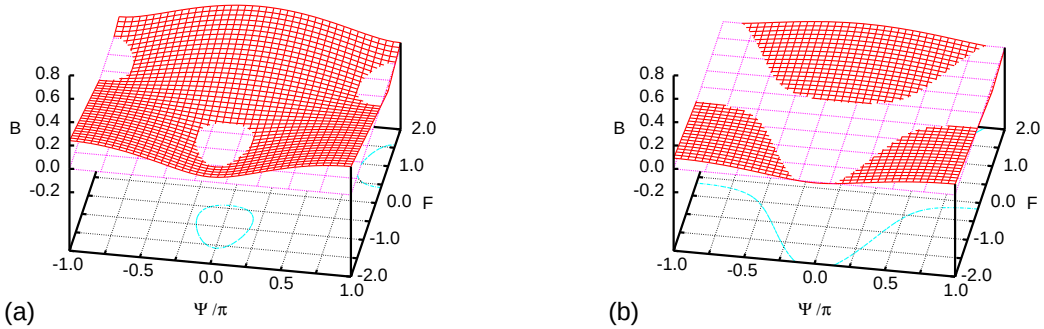

Fig. 3. Function $B(F, \Psi)$ for $\mu = 0.1$ (a) and 0.05 (b) respectively.

Therefore in this case the critical amplitude μ_c depends on control parameters F and Ψ:

$$\mu_c = \frac{1}{5}\frac{\delta^2\sqrt{\delta}\alpha}{\pi\omega^2\gamma}\sinh\left(\frac{\omega\pi}{\sqrt{\delta}}\right)\frac{1}{\sqrt{1 + F^2 + 2F\cos\Psi}}. \tag{21}$$

This is our principal result in this paper. In Fig. 2a we have plotted the results of μ_c for $\Psi = \pi$ and $F = -0.45$, 0.0, 0.45. Note that in case of $F = 0$ the additional weak resonant excitation is absent but for any other cases it influences the system vibrations. It can drive the system away ($F = 0.45$), or into ($F = -0.45$) the regions with a potential chaotic solution. To show the separation of regions with regular solutions and potential chaotic ones we calculated function $B(F, \Psi) \sim M(t_0)$ for a properly chosen t_0 (Eq. 15): In our case we defined B as follows:

$$B = \frac{1}{5}\frac{\delta^2\sqrt{\delta}\alpha}{\pi\omega^2\gamma}\sinh\left(\frac{\omega\pi}{\sqrt{\delta}}\right) - \mu\sqrt{1 + F^2 + 2F\cos\Psi}. \tag{22}$$

In Fig. 2b we present the corresponding nodal lines for given amplitudes $\mu =$ 0.04, 0.05, 0.06, 0.08, 0.10 and 0.15, respectively. On the other hand in Figs. 3a and b we show the B as a function of F and Ψ, for $\mu = 0.1$ and 0.05 (3a and b respectively). Note, the nodal lines separating regular region from the regions where chaotic solutions occur can be easily obtained by cross-section with $B = 0$ plane.

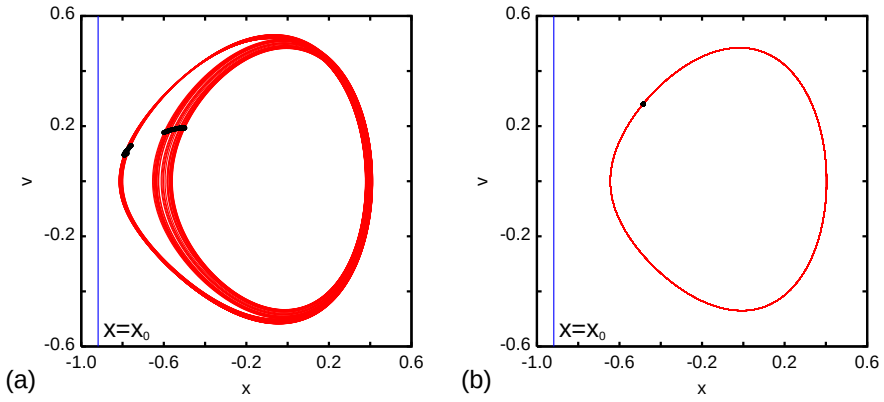

Fig. 4. Phase portraits plotted with lines together with Poincare sections denoted by points for $F = 0$ (a) and $F = 0.45$ (b). $\mu = 1$ and all other system parameter as in Fig. 2a. Note system parameters correspond to the point denoted with arrow in Fig. 2a.

4 Numerical results

To confirm the analytic predictions we have done numerical simulations for system parameters chosen as in point denoted with arrow in Fig. 2a. In Fig. 4 we have plotted phase portraits and corresponding Poincare sections for $F = 0$ (a), $F = 0.45$ (b) and $\Psi = \pi$. As expected from our initial discussion, based on approximate Mielnikov approach, we find chaotic solution in Fig. 4a. The maximal Lyapunov exponent appeared to be positive ($\lambda_1 \approx 0.05$.

On the other hand Fig. 4b shows a regular type of motion synchronised with a periodic excitation force. Note that the above numerical (Fig. 4) results confirms the analytic investigations (Fig. 2). To show the fractal structure the strange attractor (in Fig. 4a) has been also magnified in Fig. 5. Note, different range of axes in Fig. 5a-c. The characteristic double lines structure occur with the scaling factor which was estimated to be 4.

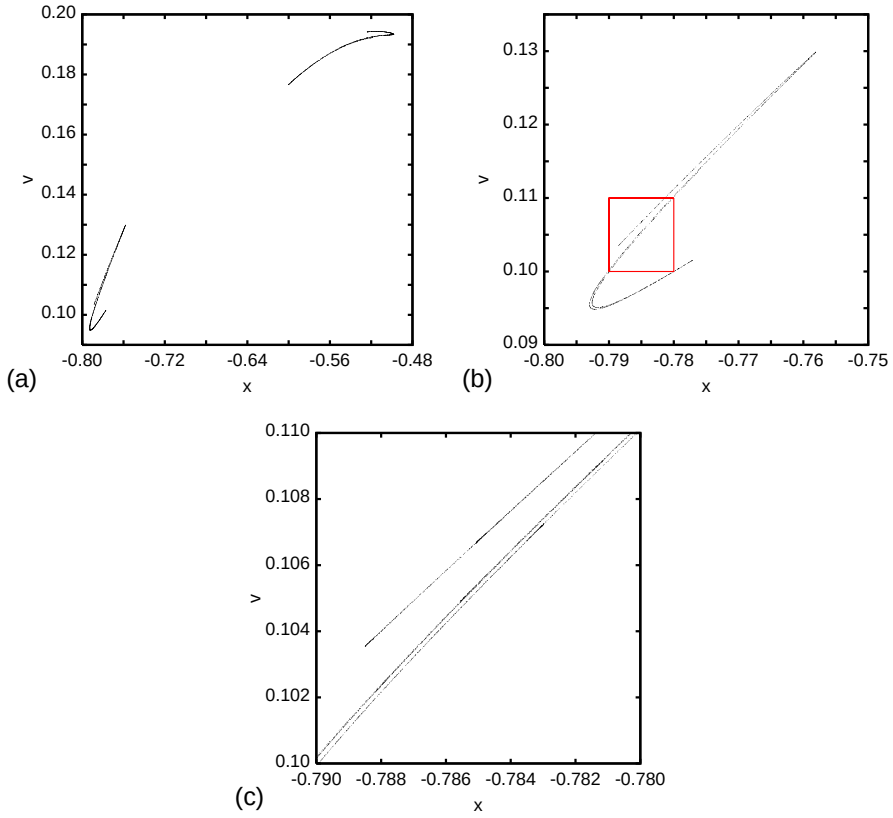

Fig. 5. (a) Chaotic attractor (magnified from Fig. 4 and its fractal structure (b-c).

5 Last remarks and conclusions

Using the Mielnikov method we have got the analytical formula for transition to chaos in a one degree of freedom, system subjected to parametric excitation with a non-symmetric stiffness with self-excitation term. Including a weak resonant term we have been able to control the type of solution. Namely it suppressed the chaotic solution by shrinking the lower bound lines of chaos in a 'phase' diagram (Fig. 2b).

In our numerical simulations of system vibration we have used the same initial conditions $x_{ini} = x_0 + 0.1$ and $v_{ini} = 0.1$ representing the point in the phase plane relatively close saddle one $(x, v) = (x_0, 0)$.

Our basic chaotic solution were very close to that one obtained by Thompson [2] with ($|\gamma| = 1.0$ and $\mu = 0.1089$). Although we have not discussed the problem of escape from the potential well we changed slightly his parameters ($\gamma \to 1.089$ and $\mu \to 0.1$) purposely. This has helped us to have more robust chaotic solution away the escape point.

In the present analysis we have used only positively defined γ and δ (see Fig. 1a). Nevertheless we claim that our results are general. Note that another choice of γ sign would only mirror our solution along the x axis ($x \to -x$). On the other hand changing $\delta \to -|\delta|$ would also rescale x axis and simultaneously shift the saddle point as well as the local minimum of the potential:

$$V(x) = -\frac{|\delta|}{2}x + \frac{\gamma}{3}x^2 = \frac{|\delta|}{6}x' + \frac{\gamma}{3}(x')^2 - \frac{1}{6}, \tag{23}$$

where $x' = x - |\delta|/\gamma$.

Acknowledgements

We would like to acknowledge partial support from Polish State Committee of Scientific Research.

Appendix A

Starting from unperturbed Hamiltonian H^0 (Eq. 5) we note that at the saddle point x_0 (Eq. 7) the system velocity is zero $v = 0$ and the energy has only its potential part

$$E = V(x = -\frac{\delta}{\gamma}) = \frac{1}{6}\frac{\delta^3}{\gamma^2}. \tag{A.1}$$

transforming Eq. 5 for chosen constant energy (Eq. A1)

$$E = \frac{1}{6}\frac{\delta^3}{\gamma^2} = \text{const} \tag{A.2}$$

we get the following expression for velocity:

$$v = \frac{\mathrm{d}x}{\mathrm{d}t} = \sqrt{2\left(\frac{1}{6}\frac{\delta^3}{\gamma^2} - \frac{\delta x^2}{2} - \frac{\gamma x^3}{3}\right)}, \tag{A.3}$$

Now one can perform integration over x

$$t - t_0 = \int \mathrm{d}x \frac{1}{\sqrt{2\left(\frac{1}{6}\frac{\delta^3}{\gamma^2} - \frac{\delta x^2}{2} - \frac{\gamma x^3}{3}\right)}}, \tag{A.4}$$

where t_0 represents an integration constant. Finally, we get so called homoclinic orbits (Fig. 1b).

$$\begin{aligned} x^* &= \frac{\delta}{\gamma}\left(\frac{1}{2} - \frac{3}{2}\tanh^2\left(\frac{\sqrt{\delta}(t-t_0)}{2}\right)\right), \\ v^* &= -\frac{3}{2}\frac{\delta\sqrt{\delta}\ \tanh\left(\frac{\sqrt{\delta}(t-t_0)}{2}\right)}{\gamma\ \cosh^2\left(\frac{\sqrt{\delta}(t-t_0)}{2}\right)}. \end{aligned} \tag{A.5}$$

References

[1] Szabelski K, Samodulski W. Drgania ukladu z niesymetryczna charakterystyka sztywnosci przy parametrycznym i zewnetrznym wymuszeniu. Mechanika Teoretyczna i Stosowana 1985;23:223–38.

[2] Thompson JMT. Chaotic Phenomena Triggering the Escape from a Potential Well. Proceedings of the Royal Society of London A 1989;421:195–225.

[3] Szabelski K. The Vibrations of Self-Excited System with Parametric Excitation and Non-Symmetric Elasticity Characteristic, Journal of Theoretical and Applied Mechanics 1991;29:57–81.

[4] Szemplińska-Stupnicka W, Rudowski J. Bifurcattions phenomena in a nonlinear oscillator: approximate analytical studies versus computer simulation results. Physica D 1993;66:368–80.

[5] Szemplińska-Stupnicka W. The analytical predictive criteria for chaos and escape in nonlinear oscillators: A survey. Nonlinear Dynamics1995;7:129–47.

[6] Rega G, Salvatori A, Benedettini F. Numerical and geometrical analysis of bifurcation and chaos for an asymmetric elastic nonlinear oscillator. Nonlinear Mechanics 1995;7:249-72.

[7] Litak G, Warmiński J, Szabelski K. Regular and chaotic vibrations of a self-excited system with parametric excitation and non-symmetric elasticity. In: proceedings of IUTAM/IFToMM Symposium on SYNTHESIS OF NONLINEAR DYNAMICAL SYSTEMS, 24-28 August 1998, Riga, Latvia. Eds. E Lavendelis and M Zakrzhevsky, Riga Technical University; Riga:1998 pp. 50–1.

[8] Rusinek R, Warmiński J, Vibrations of Rayleigh-Mathieu oscillator with quadratic elasticity characteristic. Folia Societatis Scientiarum Lublinensis 2000;9:142–51.

[9] Rand RH. Topics in nonlinear dynamics with computer algebra. Gordon and Breach; New York:1994.

[10] Rand RH, Lecture notes on nonlinear vibrations. Ithaca:The Internet-First University Press; 2003. http://www.tam.cornell.edu/randdocs/.

[11] Thompson JMT, Hunt GW. Elastic instability phenomena Wiley;Chichester:1984.

[12] Guckenheimer J, Holms P. Nonlinear Oscillations. Dynamical systems and bifurcations of vectorfields. Springer;New York:1983.

[13] Wiggins S. Introduction to applied nonlinear dynamical systems and chaos. Spinger;New York:1990.

[14] Chacon R, Palmero F, Balibrea F. Taming chaos in a driven Josephson junction, Int J. Bifurcation and Chaos 2001;11:1897–909.

[15] Cao HJ, Chi XB, Chen GR, Suppressing or inducing chaos by weak resonant excitations in an externally-forced Froude pendulum. Int. J. Bifurcation and Chaos 2004;14:1115–20.

[16] Cao HJ, Chi XB, Chen GR, Suppressing or inducing chaos in a model of robot arms and mechanical manipulators J Sound Vib. 2004;271:705–24.

[17] Litak G and Friswell MI. Nonlinear vibrations in gear systems, in: Nonlinear dynamic effects of production systems, G. Radons, R. Neugebauer (Eds.) Wiley-VCH;Weinheim:2004, pp. 331–40.